An Investigation of Tooth/Implant-Supported Fixed Prosthesis Designs with Two Different Stress Analysis Methods: An in vitro Study

TuncerBurak Özçelik, DDS, PhD;[1] and Ahmet Ersan Ersoy, DDS, PhD[2]

Purpose: Tooth/implant-supported fixed prostheses (TIFPs) present biomechanical design problems, because the implant is rigidly anchored within the alveolus, and the tooth is attached by the periodontal ligament that allows movement. While TIFP designs with rigid connectors (RCs) are preferred by many clinicians, the designs containing non-rigid connectors (NRCs) are suggested as a method to compensate for these mobility differences. However, studies have failed to show the advantage of one design over the other. This study examined stresses formed around the implant and natural tooth abutments under occlusal forces, using two dimensional finite element (2D-FEM) and photoelastic stress analysis methods (PSAM).

Materials and Methods: Connection of TIFP designs were investigated in distal extension situations using stress analysis interpreted with the 2D-FEM and PSAM. Three TIFP (screw type implant, 3.75 mm × 13 mm) models with various connection designs (i.e., rigidly connected to an abutment tooth, connected to an abutment tooth with an NRC, connected to an abutment implant with an NRC) were studied. The stress values of the three models loaded with vertical forces (250 N) were analyzed.

Results: The highest level of stresses around the implant abutment was noted on the TIFPs with the RC. On the other hand, NRCs incorporated into prostheses at the site of the implant abutment reduced the level of stresses in bone.

Conclusion: It could be suggested that if tooth and implant abutments are to be used together as fixed prostheses supports, NRCs should be placed on the implant abutment-supported site.

J Prosthodont 2007;16:107-116.

INDEX WORDS: finite element method, photoelastic stress analysis, fixed prosthesis, rigid connection, non-rigid connection

IMPLANTS may be used in two ways in the rehabilitation of partially edentulous patients: implant-supported fixed prostheses or tooth/implant-supported fixed prostheses (TIFPs).[1-3] The Branemark protocol recommends the use of the resilient restorative materials for the occlusal surfaces of the restorations and retrievable design for the prosthesis. In addition, the protocol includes the isolation of the implants from the natural teeth abutments for partially edentulous situations, due to the potential difference in the way natural teeth and implants would react to static and dynamic loading.[2]

Skalak does not recommend combining single natural tooth and ad modum Branemark implant abutments for TIFPs with rigid connectors (RCs),[4,5] since this combination of teeth and implants presents a biomechanical challenge. Indeed, oral implants are rigidly anchored into the bone and present different viscoelastic properties than the periodontal ligament around a tooth. Eventually, there are different stress and strain patterns in the bone surrounding an implant compared with a natural tooth under masticatory forces.[6-9] The clinical outcomes associated with this problem include bone resorption around the implant neck, bone fracture, fracture of attachment screws, loosening of attachment screws, cement failure, and intrusion of a natural tooth.[10-17] While a natural tooth with a healthy periodontal ligament has a mobility of 50 to 200 μm, an osseointegrated implant may move only 10 μm,

[1]Postdoctoral Fellow, Department of Prosthodontics, University of Baskent, Faculty of Dentistry, Ankara, Turkey.

[2]Professor, Department of Prosthodontics, University of Ankara, Faculty of Dentistry, Turkey.

Accepted September 26, 2005.

Correspondence to: Tuncer Burak Özçelik, Baskent Üniversitesi, Adana Uygulama ve Araştırma Merkezi Hastanesi, Diş Polikliniği, 39. Sok, No: 6, 01260 Yüreğir, Adana, Turkey. E-mail: tbozcelik@yahoo.com

1059-941X/07

doi: 10.1111/j.1532-849X.2007.00176.x

which is primarily a result of bone flexibility.[6,9,18] To compensate for these differences, the use of non-rigid connectors (NRCs),[4,12] or an implant with a stress-absorbing element (intramobile element or stress-breaking element), or an implant with a stress-eliminating space have been recommended by some authors for TIFPs.[4,7,10,19-23]

Although unequal force distribution has been demonstrated in in vitro studies, this has not usually been found to be detrimental to the implant and the surrounding tissues observed in in vivo studies.[17,24-26] However, there is disagreement in the literature on the use of RCs, NRCs, or implants with a stress-absorbing element in the TIFP. For example, McGlumphy claimed that rigid and resilient stress-absorbing elements do not take part in the stress distribution under the static loading conditions.[27] Rossen et al also reported that the variation in the E-modulus of the stress-absorbing element had no effect on the stresses in the bone.[28] Misch and Ismail compared TIFP designs with the NRC placed on the tooth side and designs with an RC using a three-dimensional finite element stress analysis (3D-FEM) and found no differences between the two models.[29] In addition, Melo et al stated that the use of NRCs in the TIFP did not result in any reduction of stress in the surrounding bone.[30] In their in vitro study, Menicucci et al found that static loading is more harmful than the transitional loads, and they concluded that the periodontal ligament plays the key role in the force distribution between a tooth and a rigidly connected implant.[31]

On the other hand, the role of the NRCs between the natural tooth and implant—especially the location of the NRC (i.e., site of the natural tooth or site of the implant)—has not been studied in detail.

In this in vitro study, it is hypothesized that various connection designs in the TIFPs may change the load transfer between implant and tooth abutments. Therefore, the purpose was to examine the stress distribution on the supporting structures of the TIFPs under static vertical loads with the 2D-FEM and the photoelastic stress analysis methods (PSAM).

Materials and Methods

In our study, TIFP designs for a case of distal extension partially edentulous mandible were evaluated. Three models, each with a different FP design, were prepared for 2D-FEM and PSAM (Table 1).

Table 1. Fixed Prosthesis Designs Used in this Study

	Fixed Prosthesis Designs
Model 1	The second premolar and the implant are connected rigidly
Model 2	The second premolar and the implant are connected by a non-rigid attachment with the matrix connector positioned on the distal side of the second premolar
Model 3	The second premolar and the implant are connected by a non-rigid attachment with the matrix connector positioned on the mesial side of the implant

It was assumed that first and second molars were lost in 2D-FEM and PSAM models and the implant (3.75 × 13, Paragon, SBM, Core-Vent, Las Vegas, NV) was placed in the second molar region.

2D-FEM

Wheeler's measurements[32] were obtained as reference for fabricating the first and second premolar teeth. Posterior mandibular region height was determined as 23 mm, cortical bone thickness was determined as 1.5 mm, and the periodontal membrane width was accepted as 0.2 mm. The axes of natural teeth and implants in models were prepared as compatible with the Spee Curve (Fig 1).

The modeling of implants and the supporting elements was performed according to the manufacturer's manual, and general rules were applied for the preparation of natural teeth and creation of metal ceramic restorations.[33,34] Ni-Cr alloy was used as a metal substructure material (Table 2).

In designs where the attachment was placed on the tooth, heavier preparation was required to accommodate the attachment. T-123 (Metalor, Neuchatel, Switzerland) slide-type attachment, which is indicated for FP, was used as the NRC. The vertical direction length of the NRC was fixed as 5 mm for all FEM models.

The materials used for the models were evaluated as homogenous, isotropic, and linear, and the osseointegration of the implants was accepted as 100%. In the mathematical model, while the implants were directly in contact with the bone, the natural teeth had primer mobility within the borders of the periodontal membrane. Also, the matrix and the patrix surfaces of the NRC of the TIFP were allowed to vertically move on each other where their surfaces were in contact.

The model drawings were created by Marc K7.2/Mentat 2001 (MARC Analysis Research Corporation, Palo Alto, CA) and a FEM Program (Bias

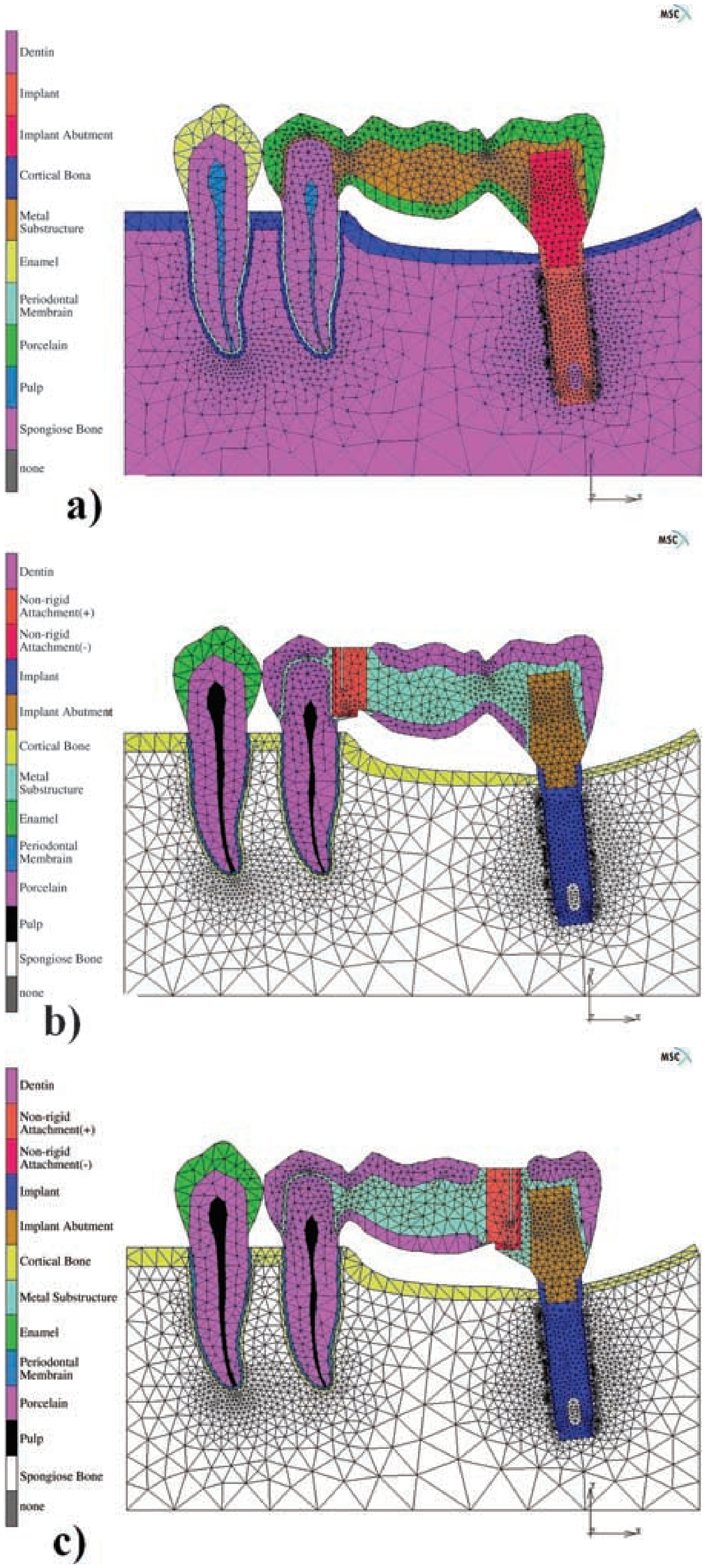

Figure 1. Models analyzed in our study. *(A)*. Model 1. The second premolar and the implant are connected rigidly. *(B)*. Model 2. The second premolar and the implant are connected by a non-rigid attachment with the matrix connector positioned on the distal side of the second premolar. *(C)*. Model 3. The second premolar and the implant are connected by a non-rigid attachment with the matrix connector positioned on the mesial side of the implant.

Electronics, Mechanical, Computer, Engineering, Consulting, Inc., Ankara, Turkey). The drawing models obtained with this process were transformed to 2D solid mathematical models with auto-mesh technique. These models were divided into triangular elements. The degree of the knot points' looseness was evaluated as three. The displacement of these points helps calculate the stress changes that occur in the structure.

Linear static analysis was performed on the prepared 2D solid models with a total masticating force of 250 N, at a right angle (0° to the long axis of supports) (Fig 2). The maximum equivalent Von Mises, which is the total value of the pressure, the tensile, and the shear tensions, was evaluated for each model on four planes (Fig 2).

2D-PSAM

The photoelastic resin (PL-2 and PLH-2, Measurements Group Inc., Raleigh, NC) used in our study was developed as a coating material for the photostress method. This material was preferred because it has often been used in the worldwide literature,[35-38] and it allows delicate evaluations due to its compatibility to 2D-PSAM.

The metal second premolars, which would be used as supports of FPs, were prepared with Ni-Cr alloy (Kera N, Eisenbacher, Dentalwaren GmbH, Autbrennlegierung, Germany) cast at average size according to the Wheeler Specifications.[32] The cast tooth supports were prepared with a chamfer 1 mm above cole. On the models where NRC (T-123, slide-type attachment, Metalor, Neuchatel, Switzerland) would be placed on the supporting cast tooth, excessive preparation was performed on the distal side of the cast tooth. A vinyl polysiloxane-based impression material with 0.2 mm thickness was used for simulating the periodontal membrane. Cemented two-piece nonrotational abutments were preferred for the implant supports. Although no preparation was performed for the two-piece non-rotational abutments, their height was standardized at 8 mm.

Table 2. Materials' Elasticity Modulus (E) and Poisson Proportions (v)

Material Properties	*Elasticity Modulus (E) (Gpa)*	*Poisson Proportion (v)*
Dentin	18.6	0.31
Implant	110	0.33
Cortical bone	15	0.30
Ni-Cr alloy	218	0.33
Enamel	84	0.33
Periodontal	2	0.45
Porcelain	69.0	0.28
Pulp	0.002	0.45
Spongiose bone	1.5	0.30
Non-rigid attachment	110	0.33

The photoelastic models were prepared according to the manufacturer's directions with width no more than 3.5 to 4 mm and with length approximately three times that of analyzed implants and metal cast teeth.

Ni-Cr alloy was used as the metal substructure for TIFP designs, which were finished with porcelain Vita 3D Master (Vita, Zahnfabrik, Bad Sackingen, Germany) using standard methods. The NRC was placed on Models 2 and 3 designs with a vertical length of 5 mm according to the manufacturer's guidelines. On Model 2, the NRC was placed with the matrix part on the distal side of the second premolar, and the patrix part was on the main body. On Model 3, the matrix part was on the implant support, and the patrix part was on the main body.

Before the loading process all photoelastic models were lubricated with machine grease for clearer images.

Each TIFP type was cemented on its own model with phosphate cement, and the models were placed and loaded on the polariscope where the stress analyses were performed. As the masticating forces in total were accepted as 250 N in our study, loading was executed at this value. Loading was performed parallel to the longitudinal axis of the implant and metal teeth supports.

As indicated in the studies of Alves et al,[39] the loading of photoelastic experimental models via opposing arch teeth would generate a more realistic load transfer. Thus the loading mechanism was formed with the same principles.

The images captured at the loading area were displayed with the aid of a digital camera (DSC-F 707, Cybershot Digital Camera, Sony, Japan)

The photoelastic stress analyses of the stress structures that occurred during loading were evaluated based on the concentration, the number, and the localization of color bands formed around supporting cast natural teeth and implants. For this reason 10 areas were defined around supporting structures (Fig 3). The stress concentration of photoelastic models was evaluated according to the values in Table 3.

Results

2D- FEM Findings

Model 1 (The second premolar and the implant are connected rigidly): The peak stress values were located

Table 3. Stress Concentration Values of the Photoelastic Models

0	No stress concentration
1	Low-level stress concentration
2	Mid-level stress concentration
3	High-level stress concentration

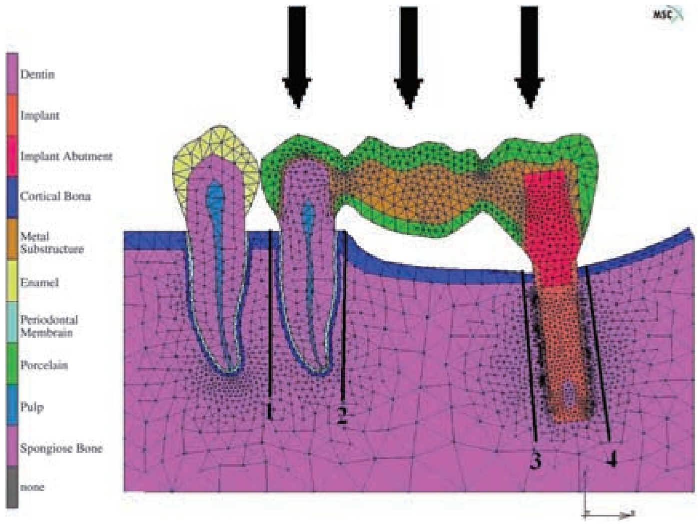

Figure 2. Black arrows show the direction of the applied load. The maximum equivalent Von Mises on the surface of bone adjacent to the natural tooth and implant was evaluated on four different planes.

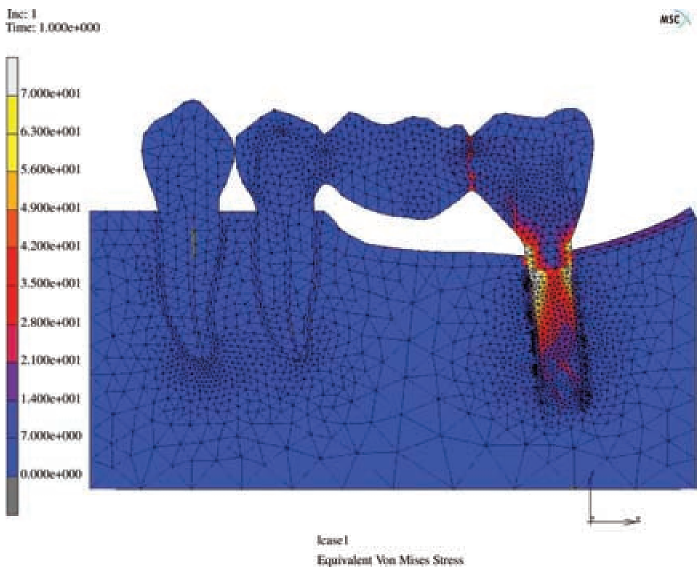

Figure 4. The stress concentration in FEM Model 1.

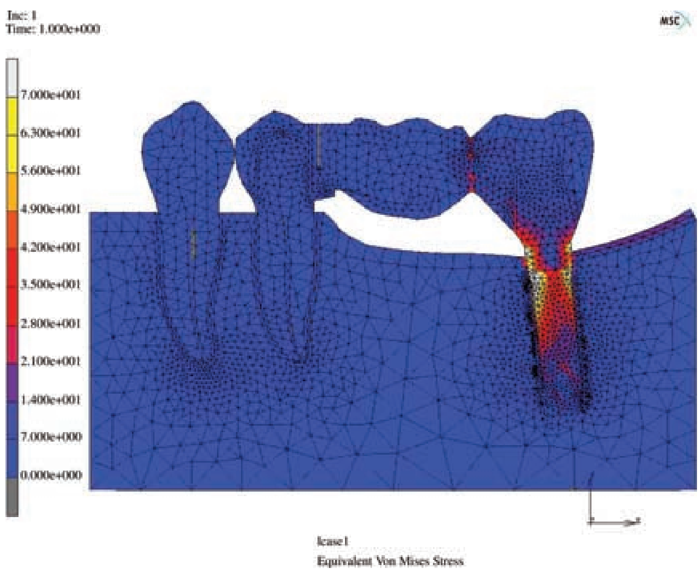

Figure 5. The stress concentration in FEM Model 2.

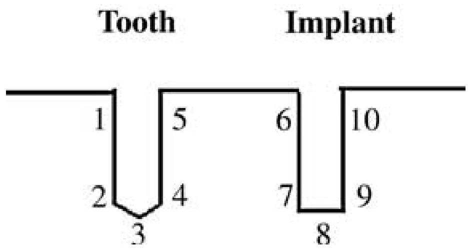

Figure 3. Simulated bone surrounding tooth and implant models was divided into ten zones to facilitate analysis of the stress patterns: Zone 1 = mesial alveolar crest, premolar; Zone 2 = mesiocervical third, premolar; Zone 3 = apical third, premolar; Zone 4 = distocervical third, premolar; Zone 5 = distal alveolar crest, premolar; Zone 6 = mesial alveolar crest, implant; Zone 7 = mesiocervical third, implant; Zone 8 = apical third, implant; Zone 9 = distocervical third, implant; and Zone 10 = distal alveolar crest, implant.

at the cortical bone region of the implant along Lines 3 and 4. The maximum stress values on the mesial and the distal crestal region of the implant bone interface was 99.04 and 89.44 MPa, respectively. The maximum stress values generated around the natural tooth were 2.778 MPa along Line 1 and 3.602 MPa along Line 2. The equivalent Von Mises stress contours for the rigid connection configuration are shown in Figure 4.

Model 2 (The second premolar and the implant are connected by a non-rigid attachment with the matrix connector positioned on the distal side of the second premolar): The highest equivalent Von Mises stress values were obtained on the cortical bone region of both the distal and the mesial sides along Lines 3 and 4 with values ranging between 97.85 and 87.91 MPa, respectively. The maximum stresses around the natural tooth were 2.935 MPa along Line 1 and 3.56 MPa along Line 2. The Von Mises stress contours for Model 2 are shown in Figure 5.

Model 3 (The second premolar and the implant are connected by a non-rigid attachment with the matrix connector positioned on the mesial side of the implant): The highest equivalent Von Mises stress values were 77.59 and 64.86 MPa, and these values were located on the cortical region of the implant abutment along Lines 3 and 4. The stresses around the natural tooth were 3.068 and 3.59 MPa along Lines 1 and 2, respectively. The equivalent Von Mises stress contours for Model 3 are shown in Figure 6.

Maximum equivalent Von Mises stress values on selected critical regions of the models are summarized in Table 4.

2D-PSAM Findings

Model 1 (The second premolar and the implant are connected rigidly): Zone 8 exhibited the largest stress magnitude around the implant abutment, followed by Zones 6 and 7. Little or no discernible stress was observed in the apical supporting areas of the tooth (Fig 7).

Model 2 (The second premolar and the implant are connected by a non-rigid attachment with the matrix connector positioned on the distal side of the second premolar): The greatest stress levels were observed in Zone 8, followed by Zones 6 and 7. These stress patterns were similar to Model 1. Very little stress concentration was observed in Zone 3, which represented the apical area of the tooth (Fig 8).

Model 3 (The second premolar and the implant are connected by a non-rigid attachment with the matrix connector positioned on the mesial side of the implant): Compared with Models 1 and 2, generally, Model 3 concentrated less stress in Zone 8. While a small reduction of stress concentration was noted in Zone 8, no changes of stress pattern were noted in any other area of the implant support. Consequently, a more uniform stress distribution was seen in this model (Fig 9).

Two-dimensional photoelastic model analysis results are presented in Table 5.

Discussion

PSAM and FEM models have been used extensively to study the biomechanics of stress transfer in dentistry; however, both methods have some limitations inherently. In PSAM, the resin which is used to simulate bone has different homogeneity and isotropic characteristics than does actual bone. In addition, the Ni-Cr alloy and the vinyl polysiloxane-based impression material cannot accurately act as a natural tooth in its periodontal ligament. The FEM program used in this investigation also has several limitations with respect to the unrealistic simulation of material properties of the structure. The program assumes that the bone, the tooth, and the periodontal ligament are homogeneous, linear-elastic, and isotropic. Furthermore, both methods assume that the bonding of the bone and the implant is perfect and all static mastication forces applied to FPDs were loaded axially in this study. However, the mastication forces are dynamic and oblique relative to the

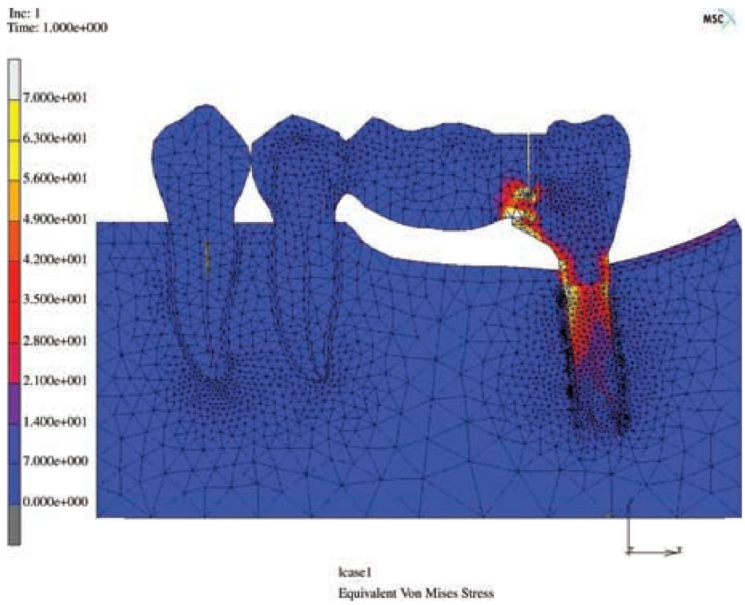

Figure 6. The stress concentration in FEM Model 3.

occlusal surface of TIFPs, and the interference between the implant and the bone is dynamic in reality. Consequently, it is usually impossible to reproduce all the details of natural behavior. Due to these limitations, the values obtained in this study may not resemble actual values but, at most, these may show the stress differences and advantages of various TIFP designs.

In the 2D system, it is assumed that out-of-plane deformations, strains, and stresses are negligible. This may reduce the cost of analysis, but it also introduces more error due to the assumed artificial boundary conditions.[40] Recently, 3D models have been preferred because more realistic results can be obtained.[29,31,40-44] To date, the 2D method has been used when numerous, varied models and designs are evaluated in the literature.[30,35,39,45-50] As many models and designs were analyzed in this study, we decided to use the 2D models for both methods.

Table 4. Von Mises Stresses at Critical Regions (MPa) with Vertical Loading of 2D FEM Models

	Natural Tooth (MPa)		*Implant Abutment (MPa)*	
	Line 1 (mesial)	*Line 2 (distal)*	*Line 3 (mesial)*	*Line 4 (distal)*
Model 1	2.778	3.602	99.04	89.44
Model 2	2.935	3.56	97.85	87.91
Model 3	3.068	3.59	77.59	64.86

In our study both similarities and differences between PSAM and FEM models were found in the stress areas around the implant support. With FEM models, the force distribution opposite the vertical forces was transmitted to the bone along the long axis of the implant, and the distribution was intensive in the mesiocervical area, descending apically. Maximum stress values intensified in the surrounding cortical bone of the implant support neck area, especially up to the first 7th and 8th grooves of the implant. Unlike FEM models, we observed that the maximum stress formed in the mesiocervical (first 3 and 4 grooves) and apical area (last six and seven grooves) of the implant supports in the PSAM models. A possible reason for maximum stress formation in mesiocervical and apical areas of the implant supports could be that photoelastic resin material, which simulates bone in the PSAM models, has a homogeneous structure. However, with the FEM models, the alveolar bone is formed by two different structures (i.e., cortical and spongious) with different elastic moduli.

We observed stress increase on the mesiocervical surface of the implant supports with all TIFP designs in both PSAM and in FEM models. The implants' movement in alveolus is at the micron level due to the rigid anchorage between bone and implant.[18,23,51] While masticating forces intrude the natural tooth into alveolus, they may cause stresses with the implant supports. Compared with natural teeth, implants' rotation center is

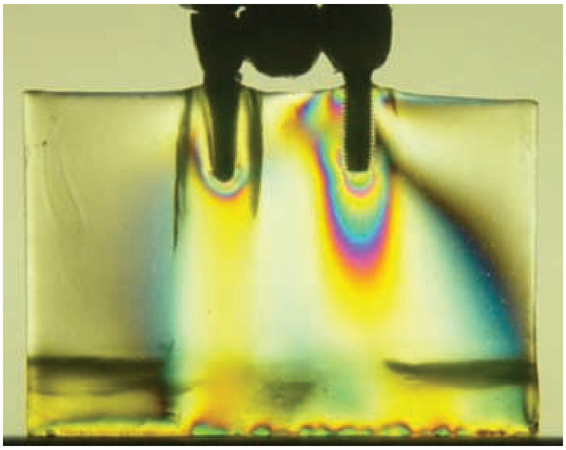

Figure 7. The stress concentration in photoelastic Model 1.

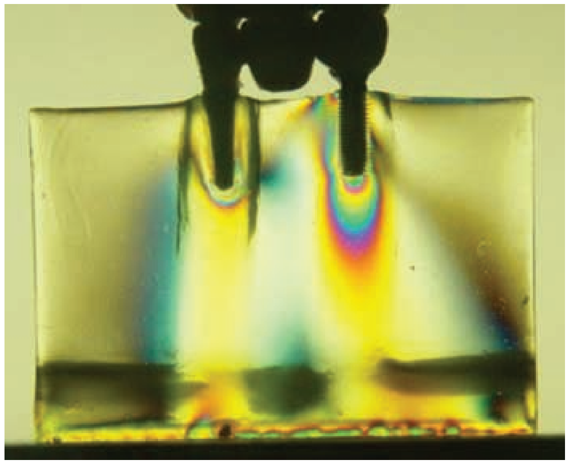

Figure 9. The stress concentration in photoelastic Model 3.

much higher—at the crestal bone level. Therefore, the stress accumulation occurs in the cortical bone area, due to the movement of the implant around this rotation center. Another reason stresses accumulate in this area is the formation of the supporting bone tissue by two structures – cortical and spongious plates, which have different elastic moduli — and the location of more rigid cortical bone on the outer surface.

No significant stress distribution differences were observed between Models 1 and 2 designs in both the PSAM and the FEM models. These results are compatible with previous studies. Breeding et al evaluated different TIFP designs and reported

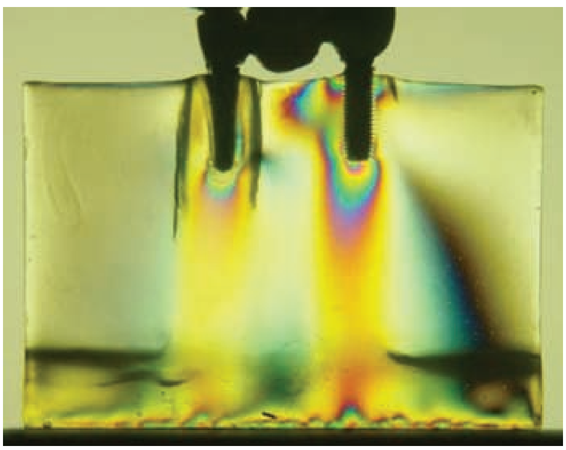

Figure 8. The stress concentration in photoelastic Model 2.

no differences between the TIFP designs with the RC and the NRC that were placed on the natural tooth side.[51] Misch and Ismail also had similar results with 3D FEM analysis.[29]

Bechelli suggested that the NRC should be placed on the implant support side with the TIFP designs to protect the implant from torque effects. He also indicated that this design has many advantages, such as allowing the physiological movements of the natural tooth, the equal distribution of forces on the implant and natural tooth, and the protection of the implant from torque effect. In addition, if the mobility of the natural tooth increases due to periodontal problems or extraction is needed, this will not affect the implant, which will be ready to use for an FP.[12] These recommendations are consistent with our study, in which a decrease in the stress formed on the implant side was observed with both PSAM and FEM models of Model 3 designs. On the other hand, with vertical loading in both PSAM and FEM models, stresses formed on the mesiocervical area of implant support were higher compared with the distocervical area in all three designs. In other words, although lower stress values were noted in Model 3 design compared with Models 1 and 2 designs, stress accumulation on the mesiocervical region of the implant support did not disappear completely, and therefore, the forces applied to TIFPs were not equally distributed onto the supports.

Table 5. Stress Values of Vertical Loading in All Designs

	Natural Tooth					*Implant Abutment*				
	Zone 1	*Zone 2*	*Zone 3*	*Zone 4*	*Zone 5*	*Zone 6*	*Zone 7*	*Zone 8*	*Zone 9*	*Zone 10*
Model 1	0	0	1	0	0	2	1	3	0	1
Model 2	0	0	1	0	0	2	1	3	0	1
Model 3	0	0	1	0	0	1	1	3	0	0

Conclusions

Within the limitations of this study, the following conclusions were drawn:

1. In both the FEM models and the PSAM models, no differences of stress distribution were observed between the non-rigid design where the non-rigid attachment was placed on the natural tooth side (Model 2) and the rigidly attached design (Model 1).
2. In the FEM models and the PSAM models where the non-rigid attachment was placed on implant support (Model 3), a decrease was noted in the stresses on the implant support.
3. Different TIFP designs did not affect the stresses formed around the natural tooth.

As a result of our study, it could be suggested that if both natural tooth and implant were used as supports for FPDs, the non-rigid attachment should be placed on the implant-supported side.

Acknowledgments

This in vitro study was supported by Research Fund of Ankara University (Project Number: 99-02-00-02).

The authors also would like to thank Associate Professor M. Cenk Haytac, Department of Periodontology, Faculty of Dentistry, University of Çukurova, for valuable suggestions for improving the presentation of this study.

References

1. Langer B, Sullivan DY: Osseointegration: its impact on the interrelationship of periodontics and restorative dentistry: Part II. Int J Periodontics Restorative Dent 1989;9:165-183
2. Kay HB: Free-standing versus implant-tooth-interconnected restorations: understanding the prosthodontic perspective. Int J Periodontics Restorative Dent 1993;13:47-69
3. Parel SM: Prosthesis design and treatment planning for the partially edentulus implant patient. J Oral Implantol 1996;22:31-33
4. Skalak R: Aspects of biomechanical considerations. In: Branemark PI, Zarb GA, Albrektsson T (eds): Tissue-Integrated Prostheses: Osseointegration in Clinical Dentistry. Chicago, IL, Quintessence, 1985, pp. 117-128
5. Skalak R: Osseointegration biomechanics. J Oral Implantol 1986;12:350-356
6. Richter EJ: Basic biomechanics of dental implants in prosthetic dentistry. J Prosthet Dent 1989;61:602-609
7. Weinberg LA, Kruger B: Biomechanical considerations when combining tooth-supported and implant-supported prostheses. Oral Surg Oral Med Oral Pathol 1994;78:22-27
8. Glantz PO, Nilner K: Biomechanical aspects of prosthetic implant-borne reconstructions. Periodontol 2000 1998;17:119-124
9. Lundgren D, Laurell L: Biomechanical aspect of fixed bridgework supported by natural teeth and endosseous implants. Periodontol 2000 1994;4:23-40
10. Babbush CA: Dental Implants: Principles And Practice. Philadelphia, PA, Saunders, 1991, pp. 67-73
11. Cho GC, Chee WW: Apparent intrusion of natural teeth under an implant-supported prosthesis: a clinical report. J Prosthet Dent 1992;68:3-5
12. Bechelli AH: The osseointegrated prosthesis—combination of osseointegrated implants and natural teeth in fixed prostheses. J Oral Implantol 1992;18:62-65
13. Sheets CG, Earthman JC: Tooth intrusion in implant-assisted prostheses. J Prosthet Dent 1997;77:39-45
14. Garcia LT, Oesterle LJ: Natural tooth intrusion phenomenon with implants: a survey. Int J Oral Maxillofac Implants 1998;13:227-231
15. Schlumberger TL, Bowley JF, Maze GI: Intrusion phenomenon in combination tooth-implant restorations: a review of the litrature. J Prosthet Dent 1998;80:199-203
16. Naert I, Quirynen M, van Steenberghe D, et al: A six-year prosthodontic study of 509 consecutively inserted implants for the treatment of partial edentulism. J Prosthet Dent 1992;67:236-245
17. Naert IE, Duyck JA, Hosny MM, et al: Freestanding and tooth-implant connected prostheses in the treatment of partially edentuluous patients. Part II. An up to 15-years radiographic evaluation. Clin Oral Implants Res 2001;12:245-251
18. Langer B, Rangert B: Biomechanical interaction between implants and teeth. In: Nevins M, Mellonig JT (eds): Implant Therapy: Clinical Approaches and Evidence of Success, vol 2. Chicago, IL, Quintessence, 1998, pp. 47-51
19. Rigdon TF: Retrievable/fixed prosthetics for implant and natural dentitions. Int J Oral Implant 1991;8:59-62

20. el Charkawi HG, Zekry KA, el Wakad MT: Stress analysis of different osseointegrated implants supporting a distal extension prosthesis. J Prosthet Dent 1994;72:614-622
21. Uysal H, İplikçioğlu H, Avci M, et al: Efficacy of the intramobile connector in implant-tooth supported fixed prostheses: an experimental stress analysis. Int J Prosthodont 1996;9:355-361
22. Lındh T, Gunne J, Danıelsson S: Rigid connections between natural teeth and implants: a technical note. Int J Oral Maxillofac Implants 1997;12:674-678
23. Becker CM, Kaiser DA: Implant-retained cantilever fixed prosthesis: where and when. J Prosthet Dent 2000;84:432-435
24. Kronström M, Trulsson M, Söderfeldt B: Patient evaluation of treatment with fixed prostheses supported by implants or a combination of teeth and implants. J Prosthodont 2004;13:160-165
25. Lang NP, Pjetursson BE, Tan K, et al: A systematic review of the survival and complication rates of fixed partial dentures (FPDs) after an observation period of at least 5 years. II. Combined tooth-implant-supported FPDs. Clin Oral Implants Res 2004;15:643-653
26. Gunne J, Astrand P, Lindh T, et al: Tooth-implant and implant supported fixed partial dentures: a 10-year report. Int J Prosthodont 1999;12:216-221
27. McGlumphy EA, Campagni WV, Peterson LJ: A comparison of the stress transfer characteristics of a dental implant with a rigid or a resilient internal element. J Prosthet Dent 1989;62:586-593
28. van Rossen IP, Braak LH, Putter C, et al: Stress-absorbing elements in dental implants. J Prosthet Dent 1990;64:198-205
29. Misch CM, Ismail YH: Finite element stress analysis of tooth-to-implant fixed partial denture designs. J Prosthodont 1993;2:83-92
30. Melo C, Matsushita Y, Koyano K, et al: Comparative stress analyses of fixed free-end osseointegrayed prostheses using the finite element method. J Oral Implantol 1995;21:290-294
31. Menicucci G, Mossolov A, Mozzati M, et al: Tooth–implant connection: some biomechanical aspects based on finite element analyses. Clin Oral Implants Res 2002;13:334-341
32. Wheeler RC: Dental Anatomy, Physiology and Occlusion (ed 5). Philadelphia, PA, Saunders, 1974.
33. Naylor WP: Introduction to Metal Ceramic Technology. Chicago, IL, Quintessence, 1992.
34. Shillingburg HT, Hobo S, Whitsett LD, et al: Fundamentals of Fixed Prosthodontics (ed 3). Chicago, IL, Quintessence, 1997.
35. Moulding MB, Holland GA, Sulik WD: Photoelastic stress analysis of supporting alveolar bone as modified by non-rigid connectors. J Prosthet Dent 1988;59:263-274
36. Pezzoli M, Highton R, Caputo A, et al: Retenion magnets in guiding plates of distal-extension removable partial dentures. J Prosthet Dent 1988;60:577-582
37. Wang CH, Tsai CC, Chen TY, et al: Photoelastic stress analysis of mandibular posterior cantilevered pontic. J Oral Rehabil 1996;23:662-666
38. Nishimura RD, Ochiai KT, Caputo AA, et al: Photoelastic stress analysis of load transfer to implants and natural teeth comparing rigid and semirigid connectors. J Prosthet Dent 1999;81:696-703
39. Alves ME, Askar EM, Randolph R, et al: A photoelastic study of three-unit mandibular posterior cantilever bridges. Int J Periodontics Restorative Dent 1990;10:153-167
40. DeTolla DH, Andreana S, Patra A, et al: Role of the finite element model in dental implants. J Oral Implantol 2000;26:77-81
41. Awadalla HA, Azarbal M, Ismail YH, et al: Three-dimensional finite element stress analysis of a cantilevered fixed partial denture. J Prosthet Dent 1992;68:243-248
42. Lozada JL, Abbate MF, Pizzarello FA, et al: Comparative three-dimensional analysis of two finite-element endosseous implant desing. J Oral Implantol 1994;20:315-321
43. Papavasiliou G, Kamposiora P, Bayne SC, et al: Three-dimensional finite element analysis of stress-distrubition around single tooth implants as a function of bony support, prosthesis type, and loading during function. J Prosthet Dent 1996;76:633-640
44. Meijer HJ, Starmans FJ, Steen WH, et al: A three-dimensional finite element study on two versus four implants in an edentulous mandible. Int J Prosthodont 1994;7:271-279
45. Tuncelli B, Poyrazoğlu E, Köylüoğlu AM, et al: Comparison of load transfer by implant abutments of various diameters. Eur J Prosthodont Restor Dent 1997;5:79-83
46. Tuncelli B, Poyrazoğlu E, Köylüoğlu AM, et al: Comparison of load transfer by angulated, standard and inclined implant abutments. Eur J Prosthodont Restor Dent 1997;5:85-88
47. Deines DN, Eick JD, Cobb CM, et al: Photoelastic stress analysis of natural teeth and three osseointegrated implant designs. Int J Periodontics Restorative Dent 1993;13:540-549
48. Holmgren EP, Seckinger RJ, Kilgren LM, et al: Evaluating parameters of osseointegrated dental implants using finite element analysis—a two dimensional comparative study examining the effects of implant diameter, implant shape and load direction. J Oral Implantol 1998;24:80-88
49. Kenney R, Rıchards MW: Photoelastic stress patterns produced by implant-retained overdentures. J Prosthet Dent 1998;80:559-564
50. Akpınar I, Anıl N, Parnas L: A natural tooth's stress distrubition in occlusion with a dental implant. J Oral Rehabil 2000;27:538-545
51. Breedıng LC, Dixon DL, Sadler JP, et al: Mechanical considerations for the implant tooth-supported fixed partial denture. J Prosthet Dent 1995;74:487-492